Miscible displacements in capillary tubes: Effect of a preexisting wall film

Ching-Yao Chen[a)]
Department of Mechanical Engineering, National Yunlin University of Science & Technology, Yunlin, Taiwan 640, Republic of China

Eckart Meiburg
Department of Mechanical and Environmental Engineering, University of California at Santa Barbara, Santa Barbara, California 93106

(Received 7 July 2003; accepted 5 November 2003; published online 26 January 2004)

For miscible displacements in capillary tubes, the impact of a preexisting wall film on the tip velocity of the displacing fluid finger is analyzed by means of axisymmetric Stokes simulations. The wall film is assumed to have the same viscosity as the displacing fluid, which is less viscous than the displaced fluid. The finger of the displacing fluid is seen to move in a quasisteady fashion, with a tip velocity below the centerline velocity of an equivalent Poiseuille flow. The explanation for this behavior, which is in contrast to our earlier findings for miscible displacements without wall films, lies in the lubricating effect of the wall film. The condition is established for which the displaced fluid moves in a nearly solid body-like motion. In this limit, a closed expression is derived for the finger tip velocity. A comparison between the simulation data and the closed form results shows reasonable agreement, provided that the criterion for solid body-like motion is satisfied. Furthermore, results are presented for the practically relevant limit of large viscosity ratios. © *2004 American Institute of Physics.* [DOI: 10.1063/1.1640373]

I. INTRODUCTION

Our interest lies in clarifying the potential role of surface tension-like stresses associated with miscible interfaces (Korteweg,[1] Davis,[2] Joseph and Renardy[3]). Neither the mathematical form of these stresses nor their magnitude is presently known to within acceptable accuracy. At the same time, there are numerous applications, ranging from a variety of chemical processes to miscible flows in porous media, in which they are potentially relevant. Consequently, there is a strong motivation to explore the nature of these stresses in some depth. For this purpose, we have been carrying out detailed experimental (Petitjeans and Maxworthy,[4] Kuang *et al.*[5]) and computational (Chen and Meiburg[6,7]) investigations of miscible displacements in capillary tubes. In these canonical flows, which also have served for studying immiscible fluids (Taylor,[8] Cox,[9] Reinelt and Saffman[10]), a finger of the displacing fluid travels along the tube axis in a quasisteady fashion, leaving behind a constant thickness film of the displaced fluid on the tube wall. The long term goal is to perform detailed comparisons between experiments and numerical simulations that include Korteweg stresses. By analyzing such global quantities as the finger propagation velocity and the film thickness, along with the detailed local velocity field near the finger tip, information can then be obtained on the existence of an effective interfacial stress field in the concentration boundary layer.

One significant obstacle that surfaces in this investigation is the tendency of gravitational effects to render the miscible displacement experiments fully three-dimensional, with much more complex features.[4,5] In order to keep these effects to a minimum, the experiments have employed capillary tubes with a very narrow diameter of $O(1\ \mathrm{mm})$. This small geometry, however, prevents highly resolved measurements of the velocity field in the interfacial region. Consequently, our combined experimental–computational group is currently preparing a set of space-based experiments that will suppress any significant gravitational effects even in wider tubes, and thereby maintain axisymmetric flow to a high degree of accuracy. For obvious reasons, this set of experiments will have to be conducted in a compact facility, and it will have to be fully automated. As a result, displacements involving many different fluid pairs will have to be carried out successively within the same tube. In between experiments, the tube will have to be cleaned of the old fluids. Since the automated cleaning procedure may leave a residue of the old fluids behind on the tube walls, the question arises as to how much such a preexisting film would affect the propagation velocity of the subsequent experiment. This issue is addressed in the current study.

II. PHYSICAL PROBLEM AND GOVERNING EQUATIONS

The present computational investigation focuses on the temporal evolution of an axisymmetric miscible interface that arises in a capillary tube when an injected fluid ''1'' displaces a resident fluid ''2'' of different viscosity. The fluids are considered to be miscible with each other in all proportions. Furthermore, a film of fluid 1 is assumed to coat the interior wall of the tube at the beginning of the displacement process, as shown by the principal sketch in Fig. 1. The goal of the investigation is to assess the influence of this preex-

a)Author to whom correspondence should be addressed. Electronic mail: chingyao@yuntech.edu.tw

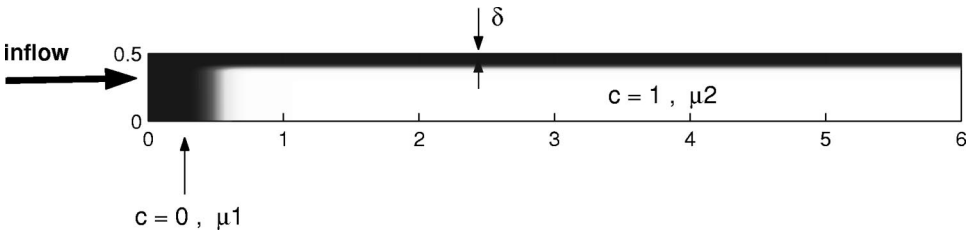

FIG. 1. Principal sketch. A less viscous fluid "1" of viscosity μ_1 is injected into a capillary tube. This tube is initially occupied by a resident core fluid "2" of larger viscosity μ_2 and a wall film of fluid 1, which is of uniform thickness δ.

isting film on the velocity with which the tip of the miscible interface advances. For the case of sufficiently slow displacements in narrow tubes, a suitably defined Reynolds number will be small, so that inertial effects can be neglected. In the absence of gravitational forces, the governing equations expressing the conservation of mass, momentum and species for simple binary mixtures hence take the form

$$\nabla \cdot \mathbf{u} = 0, \tag{1}$$

$$\nabla p = \nabla \cdot \tau, \tag{2}$$

$$\frac{\partial c}{\partial t} + \nabla \cdot (\mathbf{u}c) = D\nabla^2 c. \tag{3}$$

Here $\mathbf{u}$ denotes the velocity, p indicates the pressure, and D is the diffusion coefficient, which is assumed constant. The concentration of the displaced fluid is denoted by c. The stress tensor τ accounts for the traditional viscous stresses in Stokes flows, while any unconventional stresses, such as those postulated by Korteweg,[1] are neglected in the set of simulations to be discussed below. While we may want to include Korteweg stresses in later simulations, for now our goal is merely to evaluate the influence of a preexisting film on the basis of the Stokes equations. In order to render the governing equations dimensionless, we take the tube diameter d as the characteristic length scale. We furthermore refer all velocities to U, which denotes the centerline velocity of a Poiseuille flow with equal volume flux. All viscosities are nondimensionalized by μ_1. A pressure scale is provided by $\mu_1 U/d$. Following standard assumptions employed in the literature on miscible flows, we assume the concentration dependence of the viscosity to be of the form

$$\mu(c) = \mu_1 e^{Rc}. \tag{4}$$

Due to the axisymmetric nature of the flow, the equations can be rewritten in the streamfunction formulation as

$$\nabla^4 \psi = G(R, z, r, \psi, c), \tag{5}$$

$$\frac{\partial c}{\partial t} + \mathbf{u} \cdot \nabla c = \frac{1}{Pe} \nabla^2 c, \tag{6}$$

where G accounts for the variable viscosity terms, cf. Chen and Meiburg.[6] z and r denote the axial and radial coordinates, respectively. The Peclet number Pe is of the form

$$Pe = \frac{Ud}{D}. \tag{7}$$

We employ the same set of boundary conditions as in our earlier investigation without the preexisting wall film (Chen and Meiburg[6])

$$z = 0, L: \quad \frac{\partial^2 c}{\partial z^2} = 0, \quad \frac{\partial^2 \psi}{\partial z^2} = 0, \quad \frac{\partial^4 \psi}{\partial z^4} = 0, \tag{8}$$

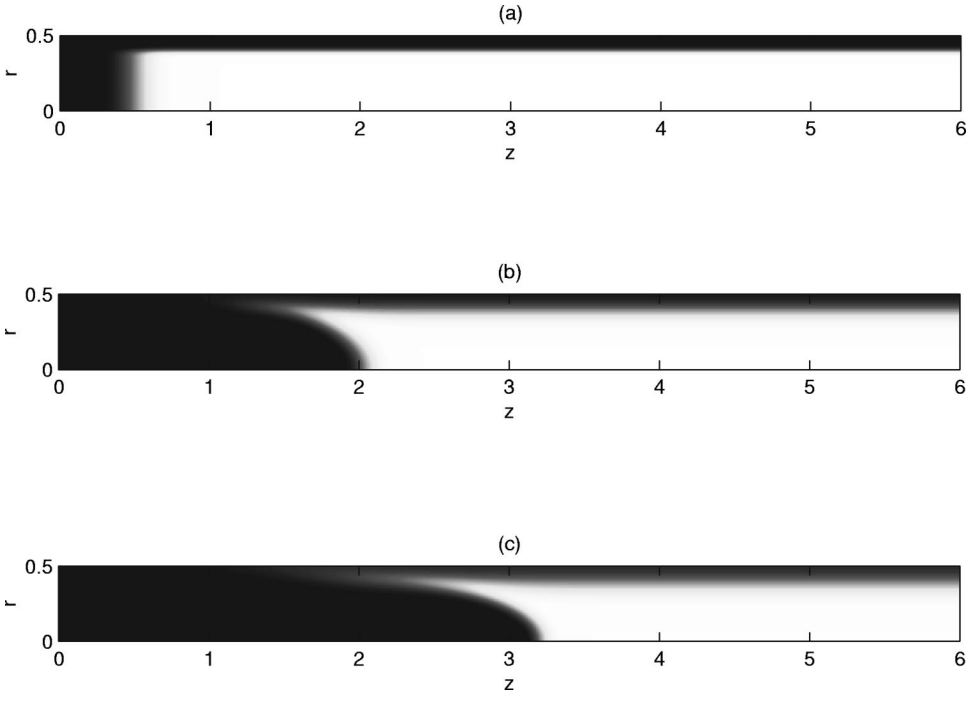

FIG. 2. Temporal evolution of the concentration field for $Pe = 1600$ and $R = 2$, with an initial wall film thickness $\delta = 0.1$: (a) Initial concentration field, (b) $t = 2$, and (c) $t = 3.5$.

$$r=0: \quad \frac{\partial c}{\partial r}=0, \quad \psi=0, \quad \frac{\partial \psi}{\partial r}=0, \tag{9}$$

$$r=0.5: \quad \frac{\partial c}{\partial r}=0, \quad \psi=1/16, \quad \frac{\partial \psi}{\partial r}=0. \tag{10}$$

Here L indicates the length of the computational domain, which typically is taken to be 6. The initial concentration field is specified as

$$c(t=0,r,z)=\int_o^z \frac{1}{\sqrt{2\pi}\sigma_z} e^{-1/2\{(z'-z_0)/\sigma_z\}^2} dz' \times \int_0^r \frac{1}{\sqrt{2\pi}\sigma_r} e^{-1/2\{(r'-r_0)/\sigma_r\}^2} dr'. \tag{11}$$

The miscible interface that initially separates the displacing from the resident fluid has a thickness of σ_z, and it is located at $z=z_0$. The preexisting wall film of fluid 1 has an initial thickness of δ, and it is separated from the core fluid 2 by a miscible layer of thickness σ_r. We conducted preliminary test calculations in order to establish that the quasisteady results to be discussed below are independent of z_0, and show only weak dependence on σ_z and σ_r, cf. also the discussion of Fig. 3 below. This independence of the initial conditions is not surprising, considering that the quasisteady long term behavior is determined by the balance of convection and diffusion. In the simulations to be discussed below, we typically employ the values $z_0=0.5$, $\sigma_z=0.1$, and $\sigma_r=0.0167$. The streamfunction equation is solved by means of a multigrid technique based on second order central differences. An alternating direction implicit (ADI) scheme (Fletcher[11]) in conjunction with third order upwind differencing is used to advance the concentration equation in time. For details, cf. Chen and Meiburg.[6] A constant time step $\Delta t=0.05$ and grid size $\Delta r=\Delta z=1/256$ are employed.

III. RESULTS

The temporal evolution of a representative flow is shown in Fig. 2. Here the Peclet number has a value of 1600, while the viscosity contrast $R=2$. The wall film thickness was set to $\delta=0.1$. We observe the formation of an axisymmetric finger of the injected fluid, which propagates towards the right along the tube axis. While most of the more viscous resident fluid is pushed downstream by the injected fluid, some of it becomes entrained in a narrow, wedge-shaped region between the injected fluid and the preexisting wall film. Figure 3 shows the propagation velocity of the finger tip as a function of time. After an initial transient, the evolution of a quasisteady state is observed, during which the finger tip velocity is nearly constant. The figure also demonstrates that the quasisteady tip propagation velocity is essentially independent of the initial conditions for σ_z and σ_r. This behavior is qualitatively similar to the situation without a wall film,[6] where we also had observed the emergence of a quasisteady state for sufficiently large values of Pe. It should be noted that a truly steady state cannot develop for miscible flows, due to the effects of diffusion on the concentration field. Figure 4 depicts the corresponding instantaneous streamline patterns in a reference frame moving with the tip velocity. A closed recirculation region is seen to form behind the finger tip, and away from the tube axis. Along the

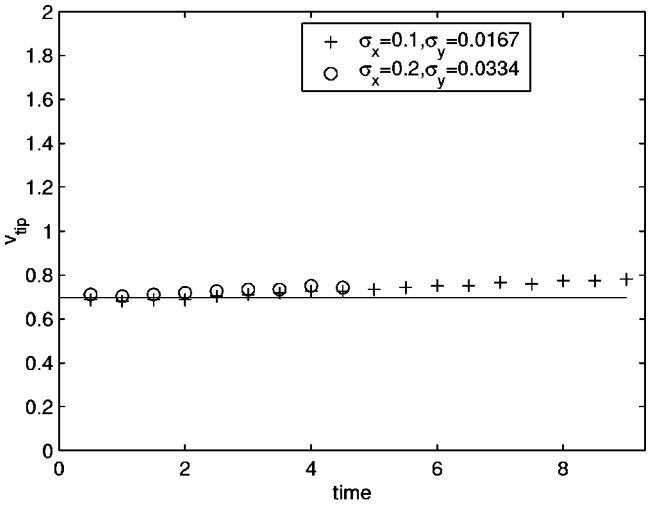

FIG. 3. Propagation velocity of the finger tip as a function of time. $Pe=1600$, $R=2$, and $\delta=0.1$. After an initial transient, the finger tip propagates with a nearly constant velocity. The symbols indicate the instantaneous velocity values, and the solid line represents a least squares fit of the data for $t\geqslant 1$.

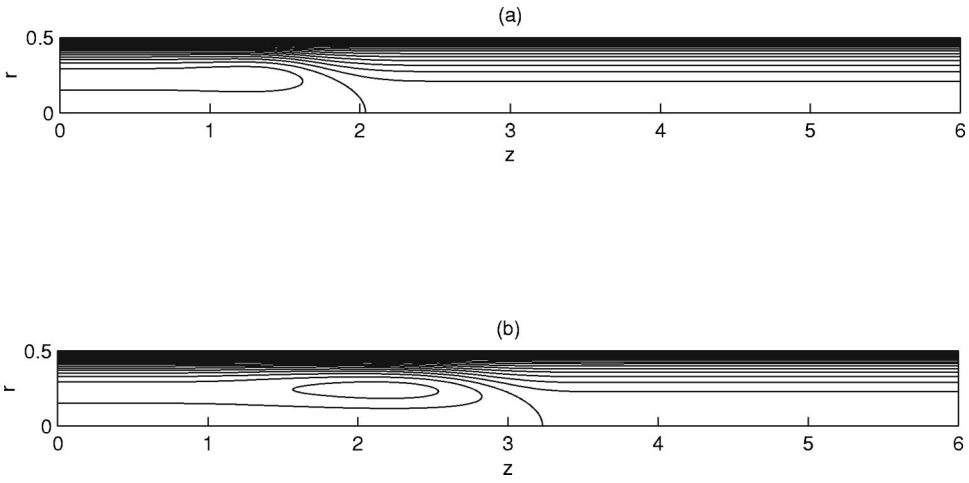

FIG. 4. Streamline pattern in a reference frame that moves with the instantaneous tip velocity, for $Pe=1600$, $R=2$, and $\delta=0.1$: (a) $t=2$ and (b) $t=3.5$. Note the formation of a closed recirculation region behind the finger tip, and away from the tube axis.

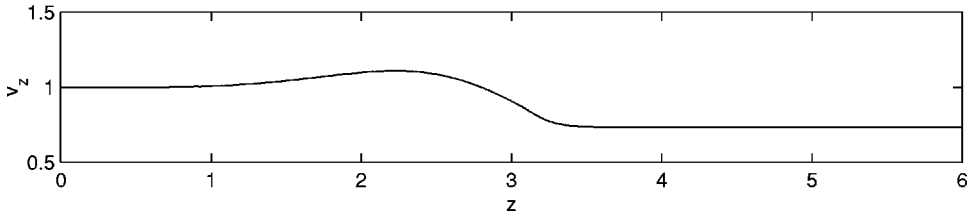

FIG. 5. $Pe=1600$, $R=2$, and $\delta=0.1$: Streamwise velocity on the axis, as a function of the axial location z, at time $t=3.5$. At this time, the finger tip is located near $z=3.5$, and it moves with a velocity $V_{tip}\approx 0.78$. Inside the finger, the streamwise velocity along the tube axis is larger than the tip propagation velocity, so that the finger tip is continuously resupplied with fresh injected fluid.

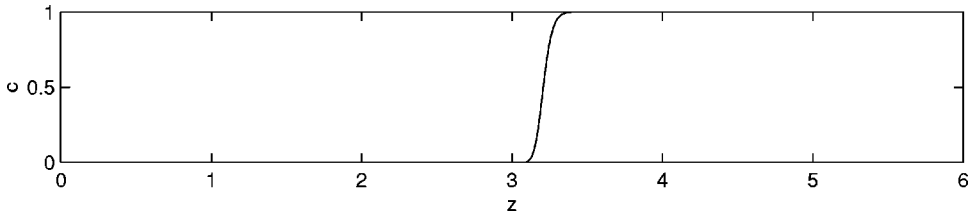

FIG. 6. $Pe=1600$, $R=2$, and $\delta=0.1$: Concentration on the tube axis, as a function of the axial location z, at time $t=3.5$. Along the tube axis, very little diffusive mixing occurs, so that the injected fluid reaches the finger tip without being significantly diluted.

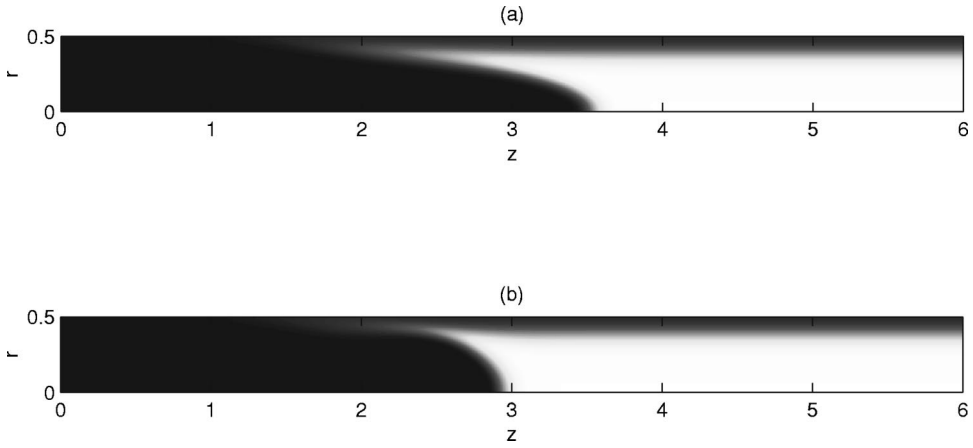

FIG. 7. $Pe=1600$, $\delta=0.1$, and $R=1$ (a) and 3 (b): Concentration fields at $t=3.5$. For the larger viscosity contrast the finger is blunter, and it propagates more slowly than for $R=1$.

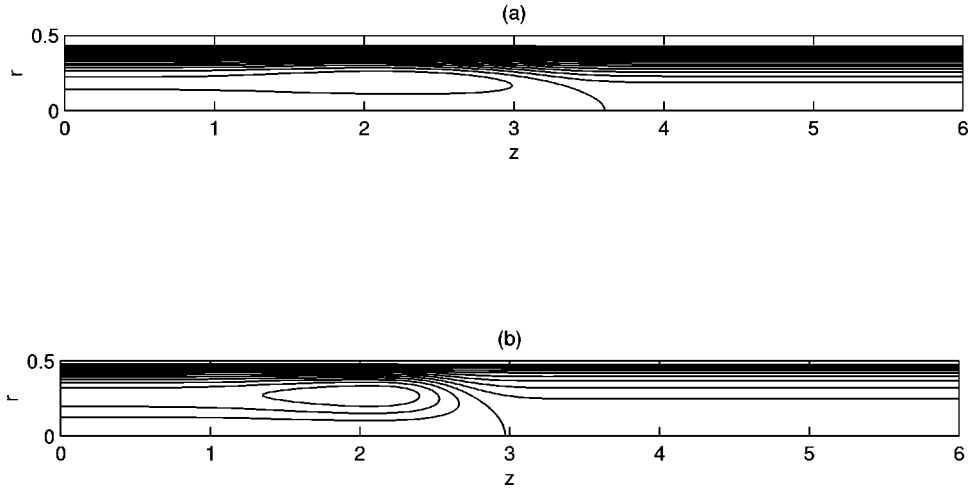

FIG. 8. $Pe=1600$, $\delta=0.1$, and $R=1$ (a) and 3 (b): Streamline patterns in the reference frame moving with the finger tip. For both R-values the finger tip velocity is below unity. However, for reasons explained in the text, the change in the streamline topology observed by Petitjeans and Maxworthy (Ref. 4) as well as by Chen and Meiburg (Ref. 6) does not occur, so that the resulting spike does not form.

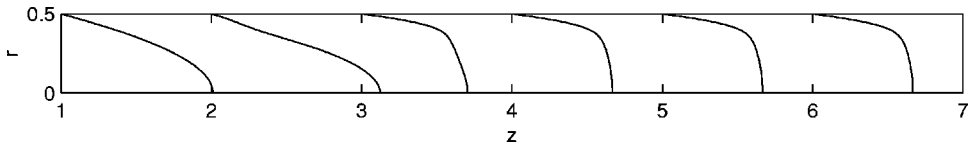

FIG. 9. $Pe=1600$, $\delta=0.1$, and $R=3$: Axial velocity profiles at various downstream locations. The less viscous wall film is seen to lubricate the more viscous core, which undergoes little deformation and moves with an approximately constant velocity.

tube axis, the injected fluid moves faster than the finger tip itself, cf. Fig. 5, so that it is brought directly to the finger tip, without any significant dilution. This is also confirmed by the concentration profile along the tube axis, shown in Fig. 6. The value of c stays very close to zero until the fluid reaches the stagnation point region at the finger tip, where a local balance exists between diffusion and the convective transport by the local strain field. Here the concentration value increases from near zero to near one in a narrow layer. Elementary scaling considerations provide an estimate of the dimensionless thickness ϵ of this layer as

$$\epsilon=\sqrt{\frac{1}{2(V_{\mathrm{tip}}-1)Pe}}, \tag{12}$$

cf. Chen and Meiburg.[6]

Figure 7 shows the fluid concentration fields for $Pe=1{,}600$, $\delta=0.1$, and $R=1$ and 3, respectively, at $t=3.5$. For the larger viscosity contrast $R=3$, the finger clearly has a blunter shape, and it propagates more slowly than for $R=1$. Note that for both R-values the finger tip propagates more slowly than a Poiseuille flow of equivalent volume flux. This is also reflected by the instantaneous streamline pattern moving with the concentration front, cf. Fig. 8. It is interesting to contrast this result with our earlier investigation of miscible displacements in vertical tubes involving fluids of certain density ratios. There we had found an interesting behavior if the finger propagated at a velocity smaller than the centerline velocity of the corresponding Poiseuille flow. In this case, since far ahead of the finger tip the velocity profile in the resident fluid is of Poiseuille type, this fluid now moves *away* from the finger tip along the centerline. This results in a topological change of the streamline pattern, which in turn produces a narrow protrusion from the finger tip that travels faster than the overall finger. Here we do not observe a corresponding behavior if the finger travels more slowly than the Poiseuille flow. The reason is that even far ahead of the finger, the flow does not acquire a Poiseuille profile. This is due to the lubrication effect of the less viscous wall film, which allows the more viscous core fluid to have a much more uniform velocity profile, with a maximum value far below one.

Interestingly, the above observation of a finger tip propagation velocity that *decreases* for increasing R, is in contrast with our earlier findings for constant density, miscible displacements without preexisting wall films, cf. Chen and Meiburg.[6] There we had observed the tip velocity to *increase* with R, while the finger width decreased. Both of these quantities were seen to reach asymptotic values as $R\rightarrow\infty$. Clearly, the existence of the wall film profoundly affects the overall character of the displacement. The lower viscosity wall film lubricates the more viscous core fluid, which tends to deform less and less for increasing viscosity contrast. For

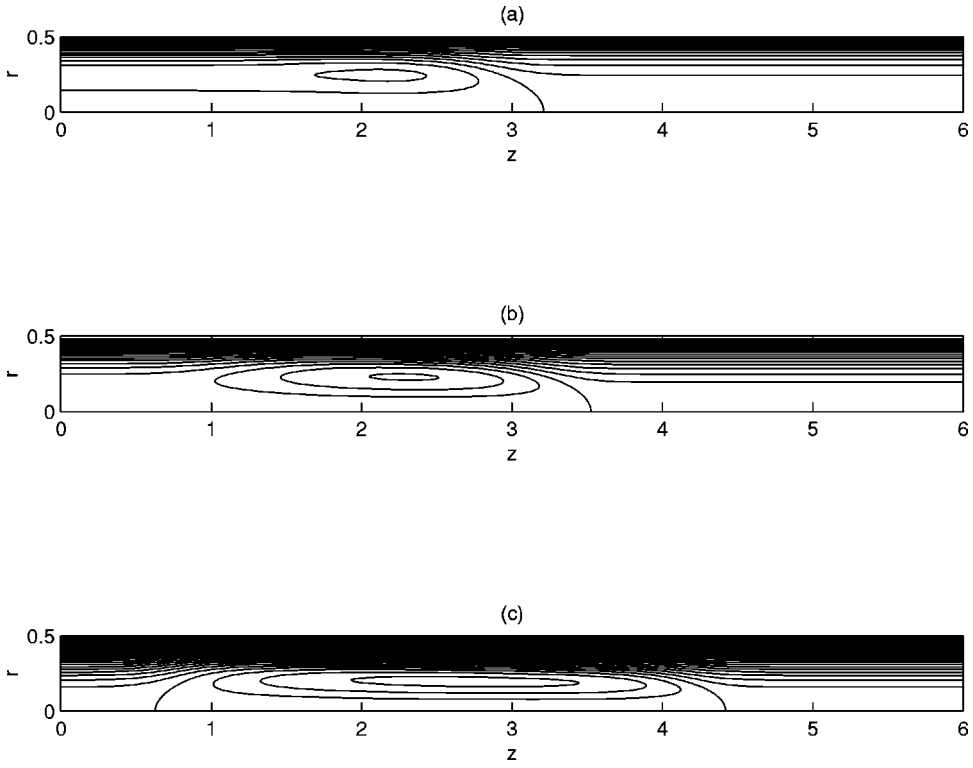

FIG. 10. Streamline patterns for $Pe=1600$, $R=2$, and $\delta=0.125$ (a), 0.05 (b), and 0 (c), in the reference frame moving with the tip. In the absence of a film on the wall (c), the velocity profile far ahead and behind the finger is of Poiseuille type, so that a closed recirculation region forms that extend from the tip of the finger to its roots.

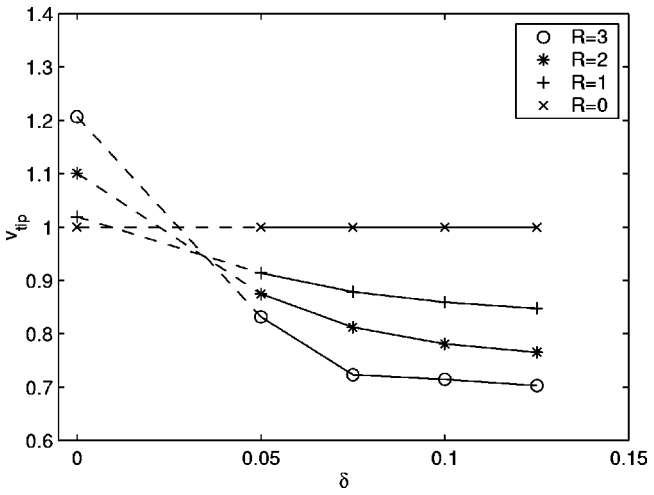

FIG. 11. Quasisteady tip velocities for $Pe=1600$ as a function of the film thickness δ, for various values of R. For films of thickness $\delta \geqslant 0.05$, small-R fingers move faster than large-R fingers, whereas in the absence of a film the opposite is true. Regarding the regime sketched by dashed lines, for which we do not have numerical data, cf. the discussion in the text.

very large viscosity ratios, the core fluid moves approximately as a solid body. This is confirmed by Fig. 9, which depicts axial velocity profiles at various downstream locations for $R=3$. It is clear that even for this moderate value of R, strong velocity gradients are limited to the wall layer, whereas the velocity remains nearly constant across the core.

The dependence of the streamline pattern, in the reference frame moving with the finger tip, on the thickness of the wall film is shown in Fig. 10. Both with and without film, the velocity profile approaches the Poiseuille form to the left of the original displacement front location. Far ahead of the finger tip, the flow is of Poiseuille type only in the absence of a film. For this reason, in this case the finger gives rise to a closed recirculation region that extends from its tip to its root. Note, however, that this closed region is not steady, but extends in length as the finger grows, so that there is a continuous inflow of fluid 1 into the recirculation region. With a film present on the wall, on the other hand, the flow ahead of the finger is not of Poiseuille type, so that a closed recirculation region forms only locally near the finger tip, and away from the axis.

Chen and Meiburg[6] had observed that, in the absence of a wall film, a large-R finger moves more rapidly than a small-R finger. In contrast, we saw above that for a film thickness of $\delta=0.1$ the exact opposite is true, i.e., the small-R finger moves faster than the large-R one. This might suggest the existence of an intermediate wall film thickness at which the tip propagation velocities of the large-R finger and the small-R finger are equal, cf. Fig. 11. We will come back to this point below. Note that for $R=0$, i.e., constant viscosity, the flow is of Poiseuille type for all film thicknesses, and the tip velocity is unity.

IV. SCALING CONSIDERATIONS

Our computational code is unable to handle film thicknesses $\delta \ll 0.05$. However, we can gain some insight into the long term behavior of such thin films on the basis of scaling arguments. The lifetime of a very thin film is limited by the diffusive growth of the transition layer that separates the film from the core fluid. In dimensionless units, this transition layer thickness σ grows as $\sqrt{t/Pe}$. The time t_c at which the transition layer has grown as thick as the film is thus given by

$$t_c = Pe\ \delta^2.$$

By this time, the finger will have reached a length of $O(Pe\ \delta^2)$. After this time, the dynamic significance of the film will decrease.

In order to establish conditions under which the core fluid will move approximately as a solid body, we focus on the purely axial flow sketched in Fig. 12, i.e., a core of fluid with viscosity μ_2 surrounded by a thin film of viscosity μ_1. We assume a sharp interface and neglect diffusive effects. The film is of thickness δ, while the core has a radius of $K=0.5-\delta$. From the no-slip condition and the balance of the tangential stresses at the interface location $r=K$ we have

$$u_1 = u_2, \tag{13}$$

$$\mu_1 \frac{du_1}{dr} = \mu_2 \frac{du_2}{dr}. \tag{14}$$

The velocity difference ΔU_1 between the wall and the interface, and the difference ΔU_2 between the interface and the centerline scale as

$$\Delta U_1 \sim \delta \frac{du_1}{dr}(r=K), \tag{15}$$

$$\Delta U_2 \sim K \frac{du_2}{dr}(r=K). \tag{16}$$

Solid body-like motion of fluid 2 exists when $\Delta U_2 \ll \Delta U_1$, i.e.,

$$R = \ln \frac{\mu_2}{\mu_1} \gg \ln \frac{K}{\delta}. \tag{17}$$

The general solution for the velocity profile is of the form

$$u_1(r) = \frac{1}{1-16K^4(1-e^{-R})}(1-4r^2), \tag{18}$$

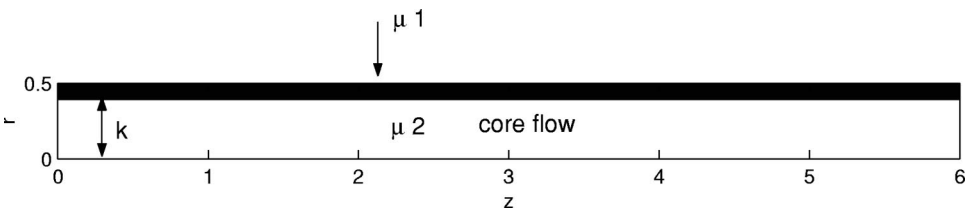

FIG. 12. One-dimensional model flow. A core of more viscous fluid "2" is surrounded by a wall film of fluid "1." The interface is located at $K=0.5-\delta$.

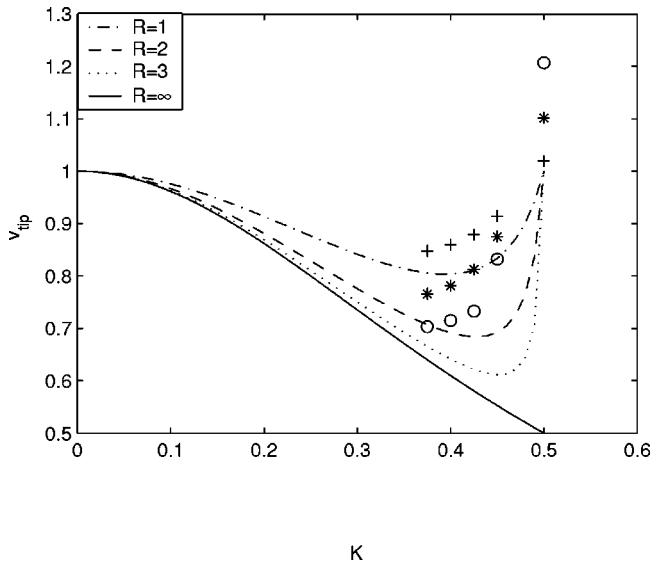

FIG. 13. The tip velocity V_{tip} as calculated from Eq. (20). The symbols refer to simulation data: $R=1$ (+), $R=2$ (*), $R=3$ (○). The solid line represents the asymptotic value for $R\to\infty$, as calculated from relationship (21). For small values of the film thickness δ, i.e., $K\to 0.5$, criterion (17) for approximate solid body motion of the more viscous fluid is not satified for the present, relatively low values of R, which explains the discrepancy between the simulation data and the theoretical curves.

$$u_2(r)=\frac{4\,e^{-R}}{1-16K^4(1-e^{-R})}(K^2-r^2)+\frac{1}{1-16K^4(1-e^{-R})}(1-4K^2). \tag{19}$$

If fluid 2 moves approximately as a solid body, i.e., if Eq. (17) is satisfied, we can approximate the finger tip velocity by $u_2(r=0)$, so that we obtain

$$V_{tip}=\frac{1-4K^2(1-e^{-R})}{1-16K^4(1-e^{-R})}. \tag{20}$$

It is immediately clear that for $R\geqslant 0$ and $K<0.5$, this estimate for V_{tip} cannot exceed the value of one. Consequently, for the assumed flow structure of a less viscous wall film and a more viscous core layer, the maximum velocity is always smaller than that of the corresponding Poiseuille profile. In order to obtain $V_{tip}>1$, a layer of the more viscous fluid would have to become entrained in a quasisteady fashion by the flow in between the finger and the wall film, so that the core fluid can no longer move in a near solid body-like way. The resulting flow would then be similar to the case without a wall layer, with the wall film becoming dynamically unimportant. In our simulations, this situation was never observed. However, we cannot exclude the possibility that for large Pe and thin wall films, such a situation could arise. Hence, the exact nature of Fig. 11 in the range $0<\delta<0.05$ cannot be resolved conclusively at this time.

Figure 13 plots the theoretical predictions of Eq. (20) for the tip velocity V_{tip}, along with the corresponding simulation data discussed earlier. For small values of the film thickness δ, i.e., $K\to 0.5$, criterion (17) for approximate solid body motion of the more viscous fluid is not satified for the present, relatively low values of R. Furthermore, diffusive effects may become important as well when the wall film is very thin. As a result, there is a significant difference between the tip velocity of the finger and the centerline velocity of the more viscous, displaced fluid far downstream of the finger. This explains the discrepancy between the simulation data and the theoretical curves. However, for larger values of δ, the agreement is seen to improve.

It is of interest to obtain the dependence of the tip velocity (20) on R and K in the limit of $R\to\infty$. From Eq. (20), we obtain

$$V_{tip}\to\frac{1}{4K^2+1}. \tag{21}$$

This result is plotted as a solid line in Fig. 13. Obviously, it is not valid right at $K=0.5$, where condition (17) is no longer satisfied.

V. CONCLUSIONS

Motivated by the need to perform an entire series of automated, miscible displacement experiments in a single capillary tube, we have addressed the impact of a preexisting wall film on the tip velocity of the displacing fluid finger. Here the wall film is assumed to have the same viscosity as the displacing fluid, which is less viscous than the displaced fluid. After an initial transient, the finger of the displacing fluid is seen to move in a quasisteady fashion. All of our axisymmetric Stokes flow simulations show the finger advancing with a velocity below the centerline velocity of an equivalent Poiseuille flow. This is in contrast to our earlier findings for displacements without preexisting wall films. The explanation is found in the lubrication effect of the wall film. We establish the condition for which the displaced fluid moves in a nearly solid body-like motion. In this limit, the finger tip velocity can be approximately evaluated in closed form from a one-dimensional model flow. A comparison between the simulation data and the closed form results is presented which shows reasonable agreement, provided that the criterion for solid body-like motion is satisfied. In addition, results are presented for the practically relevant limit of very large viscosity ratios.

ACKNOWLEDGMENTS

The authors would like to thank Tony Maxworthy for several fruitful discussions. This research is supported by the NASA Microgravity and NSF/ITR programs, by the Basic Energy Sciences program of the Department of Energy, and by the University of California Energy Institute, as well as by an NSF equipment grant. C.-Y.C. was supported by ROC NSC (Grant No. NSC 91-2212-E-212-017).

[1] D. Korteweg, "Sur la forme que prennent les équations du mouvement des fluides si l'on tient compte des forces capillaires causées par des variations de densité," Arch. Neel. Sci. Ex. Nat. (II) 6 (1901).
[2] H. Davis, "A theory of tension at a miscible displacement front," in *Numerical Simulation in Oil Recovery*, IMA Volumes in Mathematics and Its Applications 11 (Springer, New York, 1988).
[3] D. Joseph and Y. Renardy, *Fundamentals of Two-Fluid Dynamics, Part II* (Springer, New York, 1992).

[4]P. Petitjeans and T. Maxworthy, ''Miscible displacements in capillary tubes. Part 1: Experiments,'' J. Fluid Mech. **326**, 37 (1996).
[5]J. Kuang, T. Maxworthy, and P. Petitjeans, ''Miscible displacements between silicone oils in capillary tubes,'' Eur. J. Mech. B/Fluids **22**, 271 (2002).
[6]C.-Y. Chen and E. Meiburg, ''Miscible displacements in capillary tubes. Part 2: Numerical simulations,'' J. Fluid Mech. **326**, 57 (1996).
[7]C.-Y. Chen and E. Meiburg, ''Miscible displacements in capillary tubes: Influence of Korteweg stresses and divergence effects,'' Phys. Fluids **14**, 2052 (2002).
[8]G. I. Taylor, ''Deposition of a viscous fluid on the wall of a tube,'' J. Fluid Mech. **10**, 161 (1961).
[9]B. G. Cox, ''On driving a viscous fluid out of a tube,'' J. Fluid Mech. **14**, 81 (1962).
[10]D. A. Reinelt and P. G. Saffman, ''The penetration of a finger into a viscous fluid in a channel and tube,'' SIAM (Soc. Ind. Appl. Math.) J. Sci. Stat. Comput. **6**, 542 (1985).
[11]C. A. J. Fletcher, *Computational Techniques for Fluid Dynamics, Vol. 1* (Springer, New York, 1988).